

Large-scale high-resolution yearly modeling of forest growing stock volume and above-ground carbon pool

Elia Vangi ^{a,b}, Giovanni D'Amico ^{a,c,*}, Saverio Francini ^{a,d}, Costanza Borghi ^a, Francesca Giannetti ^a, Piermaria Corona ^c, Marco Marchetti ^b, Davide Travaglini ^a, Guido Pellis ^e, Marina Vitullo ^e, Gherardo Chirici ^a

^a Dipartimento di Scienze e Tecnologie Agrarie, Alimentari, Ambientali e Forestali, Università degli Studi di Firenze, Italy

^b Dipartimento di Bioscienze e Territorio, Università degli Studi del Molise, Italy

^c CREA Research Centre for Forestry and Wood, Italy

^d Fondazione per il Futuro delle Città, Firenze, Italy

^e Istituto Superiore per la Protezione e la Ricerca Ambientale, Italy



ARTICLE INFO

Keywords:

National forest inventory
GSV
Carbon stock
Forest modeling
Spatial modeling
Italy

ABSTRACT

Within the Paris Agreement's Enhanced Transparency Framework, consistent data collections are the prerequisite for a successful reporting of GHG emissions. For such purposes, NFIs are usually the primary source of information, even if they are frequently not designed for producing estimations on a yearly basis and in the form of wall-to-wall high-resolution maps. In this framework, we present a new spatial model to produce yearly growing stock volume (GSV), above-ground biomass (AGB), and carbon stock wall-to-wall estimates. We tested the model in Italy for the period 2005–2018, obtaining a time-series of yearly maps at 23 m spatial resolution. Results were validated against the 2015 Italian NFI reaching an average RMSE% of 19% for aggregated areas. Results were also compared against data reported by the Italian GHG inventory, reaching an RMSE% of 28% and 20% for GSV and carbon stock respectively.

We demonstrated that the modeling approach can be successfully used for setting up a forest monitoring system to meet the interests of governments in inventories of GHG emissions and private entities in carbon offset investments.

1. Introduction

Under the enhanced transparency framework of the Paris Agreement, each country Party must report every two years an inventory of their anthropogenic greenhouse gases (GHGs) emissions by sources and removals by sinks following the Intergovernmental Panel on Climate Change (IPCC) guidelines and guidance (IPCC et al., 2006). The GHG emission inventory has to fulfill the IPCC key principles: transparency, accuracy, completeness, consistency, and comparability while providing helpful information for assessing the climate impacts. The "Land Use, Land-Use Change and Forestry" (LULUCF) is exceptionally demanding, dealing with natural carbon dynamics and aiming to assess emissions and removals related to the impact of anthropogenic activities. The LULUCF sector is responsible for significant GHG emissions globally, mainly due to deforestation activities. In this framework, forests are pivotal ecosystems, being a substantial and growing atmospheric carbon

sink (Sellers et al., 2018). Forests are estimated to sequester 30% of the total global CO₂ released into the atmosphere annually (Houghton and Nassikas, 2017), corresponding to 7.6 Gt CO₂ y⁻¹, reflecting a balance between gross carbon removals and gross emissions from deforestation and other disturbances (Harris et al., 202; Xu et al., 2021). Increasing the carbon stored in the above and below-ground forest biomass is a mitigation mechanism to fight climate change and offset anthropogenic emissions worldwide (Di Cosmo et al., 2016).

Despite the UNFCCC requirements related to the provision by Parties of biennial forestry-related carbon stock change, many National Forest Inventories (NFI) are not designed for continuous yearly reports and cannot cope with the required reporting frequency due to longer update cycles (McRoberts et al., 2018). Estimating carbon stock changes between consecutive NFIs is a pivotal step in accomplishing the reporting requirements. The methodology should be based on year-to-year measured forest variables or prediction models to extend NFI-based

* Corresponding author. Dipartimento di Scienze e Tecnologie Agrarie, Alimentari, Ambientali e Forestali, Università degli Studi di Firenze, Italy.
E-mail address: giovanni.damico@unifi.it (G. D'Amico).

estimates to assessment years rather than a simple interpolation between estimates produced by NFIs at different years (Federici et al., 2008).

Even if the main source of information for such reporting activities are NFIs (Tomppo et al., 2010; Condés and McRoberts, 2017; Kulbokas et al., 2019), in recent times, considerable efforts have been laid out to integrate remotely sensed (RS) data in the process. Examples are available to provide spatially continuous (also referred to as wall-to-wall maps) and updated estimations of several forest variables such as: the growing stock volumes (GSV), the above-ground biomass (AGB) (Kangas et al., 2018; Chirici et al., 2020; Vangi et al., 2021), and the rate of forest disturbances (Hansen et al., 2013; van der Werf et al., 2017; Francini et al., 2021; Francini et al., 2022a, a; Francini et al., 2022b, b). Coupling traditional NFI information acquired in the field with such wall-to-wall maps based on remotely sensed data is the basis for evolving from traditional NFIs to the new so called Enhanced Forest Inventory (EFI) framework (White et al., 2016). This has already been carried out by Countries with a long history in NFIs, such as those in the Scandinavian area (Næsset et al., 2004; Nord-Larsen and Schumacher, 2012; Tomppo et al., 2008), Canada (White et al., 2016), Austria (Hollaus et al., 2009) and Switzerland (Waser et al., 2017). The EFI approach has several benefits (Chirici et al., 2020): it enables the estimation of forest attributes from a local to national scale to support local management and national planning; it can provide estimates of forest removals due to logging and other disturbances, which are essential in the context of carbon cycle assessments (Francini et al., 2021). But evolving from traditional NFIs to EFIs requires elaborating a huge amount of remotely sensed (RS) data which in turn requires investments in software and hardware resources for their processing (D'Amico et al., 2021). Conversely, field activities can be reduced by optimizing the sampling strategy by integrating RS data (Corona, 2010). For example biomass density maps constructed from remotely sensed data can be used to enhance the stratification of ground inventories, to supply carbon stock changes estimates in poorly-sampled or unapproachable areas, or for verification purposes (ISPRa, 2021a).

Coming more specifically to the problem of how to estimate forest carbon stock changes, there are at least three approaches reported in literature that are based on different level of data availability (Williams et al., 2012). The first one is the gain-loss method, a process-based approach, which estimates emissions and removals from changes in carbon stocks due to forest land and related land-use changes. Default data are provided in each land-use category chapter to allow the estimation of biomass carbon stock changes in case of missing country-specific data. This is the method recommended only for countries without an NFI and poor data collection.

In the second approach, forest carbon sinks are estimated by coupling estimates of forest age with age-specific carbon sequestration models. These models are derived from yield tables, expressing carbon stocks as a function of age stand.

The third approach, called the stock-change approach, requires bi-temporal biomass carbon stock measurements; therefore, its application is suitable in countries having NFI systems and other land-use categories, where stocks of different biomass pools are surveyed with a regular frequency. This method results in considerably less uncertainty (McRoberts et al., 2018; ISPRa, 2021a).

Examples of these approaches are presented by Harris et al. (2021) and Xu et al. (2021), they both integrated spatially explicit datasets and ground-measured forest inventories data to provide global estimates of temporally averaged global forest carbon emissions and removals for the 21st century, founding that woody carbon stocks increased slowly but significantly at a local and regional scale.

Saatchi et al. (2011) presented a benchmark map of biomass carbon content across the world's tropical forests for 2000 by combining ground data with airborne laser scanning (ALS), multispectral, and radar data: their map provided estimations of carbon stocks for countries where prior estimates were scarce or not complete. With the stock-change

approach, Paul et al. (2021) assessed the carbon stock and changes in New Zealand using the NFI data from 2002 to 2014, showing that national forests are carbon-neutral but with wide variation in carbon stocks between different forest categories. In Russia, Shepashenko et al. (2021) used multiple RS-based maps and NFI data to estimate CO₂ sequestration founding figures 47% higher than the national GHG inventory.

In Italy, Dalponte and Coomes (2016) developed an approach to map the carbon density of the Italian Alps through ALS and hyperspectral data. Nonini and Fiala (2021) developed a model to assess the forest biomass and carbon stock at stand-level with a gain-loss approach in a northern region in Italy.

Federici et al. (2008) developed a model to estimate carbon stock change data for the carbon pools to be reported under the forest land category in the LULUCF sector in the GHG inventory. The *For-est* (*Forest – estimates*) is a bookkeeping model that calculates the above-ground biomass pool C stock annually by adding the annual net increment and subtracting yearly losses associated with harvest (industrial roundwood and fuelwood), forest fires, and other mortality. A detailed description of the modeling approach is reported in Italian Ministry for the EnvironmentLand and Sea, 2019 (section 3.3). The annual GSV is converted to AGB and then to carbon stock by species-specific parameters. The model is currently used by Italy to estimate carbon stock changes for the national GHG inventory under UNFCCC (ISPRa, 2021b; b).

The aim of this study is to present the development of a spatial approach for the wall-to-wall estimation of GSV and carbon stock to fill the information gaps left by the long updating cycle of the periodic Italian NFI, under the framework for a new EFI that better fits the international reporting requirements.

To do so, we propose a new methodology to produce a yearly high-resolution (23 m) forest above-ground carbon pools and GSV maps. Our approach is initiated by a 23 m resolution wall-to-wall GSV map of 2005 constructed by combining Landsat imagery with NFI data (Vangi et al., 2021). We then applied yearly increments with species-specific growth models derived from yield tables driven by the forest GSV to estimate the annual current increment (Federici et al., 2008). We take into account removals due to forest disturbances predicted using Landsat imagery and the 3I3D forest disturbance detection algorithm (Francini et al., 2021; Francini et al., 2022a; a). The approach was tuned against a set of independent field observations, and the final pixel-level estimates were aggregated at the regional level and validated against the design-based estimation from the last Italian NFI completed in 2015, obtaining an RMSE% at a regional level of 19% and 17% for GSV and carbon stock, respectively. Our estimates were also compared with official data reported in the Italian GHG inventory.

To the best of the author's knowledge, this represents the first attempt to provide high-resolution wall-to-wall yearly time-series maps of forest growing stock volume and carbon stock in Italy. These new products allow the spatial analysis of the annual Italian forest carbon stock changes, consistently with the IPCC guidelines.

2. Materials

2.1. Study area

The study was carried out in Italy, covering 301,408 km² (Fig. 1). Italy has a wide range of climatic conditions due to its proximity to the sea and the presence of two main mountain belts with elevations ranging between sea level up to 4000 m a.s.l. Italy has mainly a temperate Mediterranean climate (Pinna, 1970). According to the 2015 Italian NFI (INFC, 2021), forest vegetation and other wooded lands occupy 11,054, 458 ha, about 36% of the national land. Deciduous species cover 68% of the forest area and are represented mainly by Quercus oak (*Q. petraea* (Matt.) Liebl., *Q. pubescens* Willd., *Q. robur* L., *Q. cerris* L.), and European beech (*Fagus sylvatica* L.). Coniferous species, such as Norway spruce

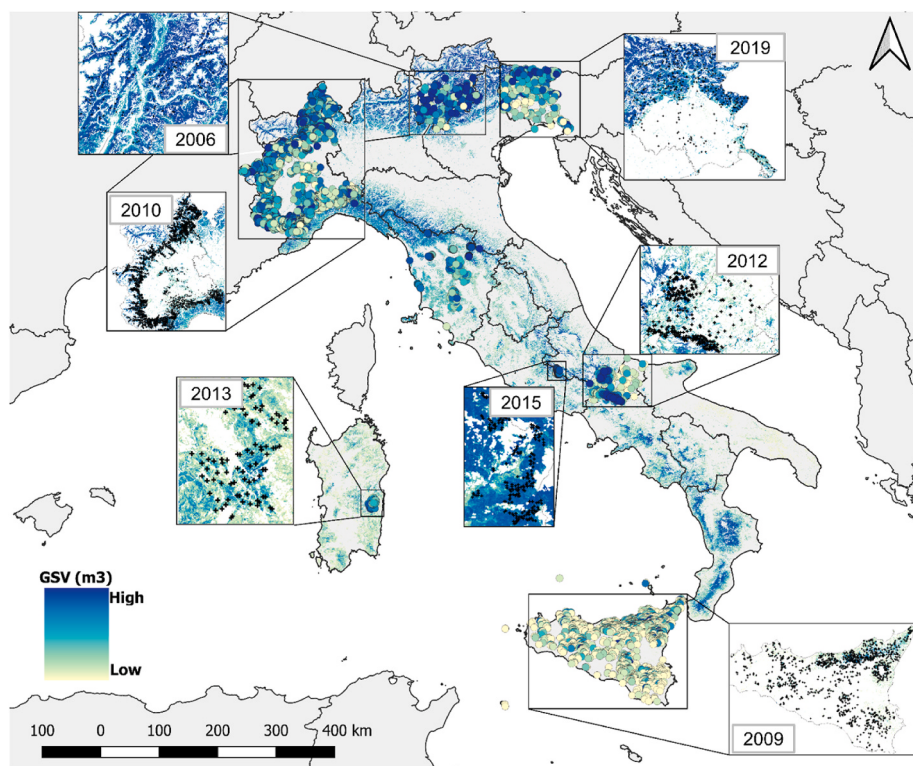


Fig. 1. The study area (the whole of Italy) with the location of the independent plots was used for optimizing and validating the model.

(*Picea abies* (L.) H. Karst.) and pines (*Pinus sylvestris* L., *P. nigra* J.F. Arnold, *P. pinæ* L., *P. pinaster* Aiton), form vast plantations, especially in the northern regions and coastal areas (Fig. 1).

Italy is divided into 20 administrative regions (NUTS2); the NFI produces every ten years regional estimates for several variables including forest area, total and average GSV, and biomass with the relative associated standard errors (SE) with a traditional design-based approach. According to NFIs, at the country level, the average GSV was $121 \text{ m}^3 \text{ ha}^{-1}$ and $135 \text{ m}^3 \text{ ha}^{-1}$ in 2005 and 2015, respectively.

2.2. Growing stock volume baseline map

For the assessment of forest GSV and above-ground carbon stock in the years following the last NFI, we used the 2005 GSV map produced by Vangi et al. (2021) for Italy as the initial GSV baseline data (GSV₂₀₀₅). This map consists of GSV predictions by Landsat and other RS imagery at $23 \times 23 \text{ m}$ resolution for all forest pixels. The full description of the methodology is available from Chirici et al. (2020). The model fitting and tuning steps were carried out using the *randomForest* package in the statistical software R 4.0.5 (Liaw and Wiener, 2002) (<https://www.r-project.org>, accessed on: June 16th, 2021). The pixel-level estimations of the GSV range between 0 and $690 \text{ m}^3 \text{ ha}^{-1}$ with a mean value of $134 \text{ m}^3 \text{ ha}^{-1}$ and a standard deviation of $41.5 \text{ m}^3 \text{ ha}^{-1}$ (for comparison the official NFI estimates range between 0 and 950 with a mean value of 145 and a standard deviation of $69 \text{ m}^3 \text{ ha}^{-1}$). Using a model-assisted estimation approach (Corona, 2010), the 2005 growing stock volume map led to a standard error of 1.2% and 1% for the mean and total national GSV estimation, respectively (Vangi et al., 2021).

2.3. Forest category maps

In Italy, a forest category map with a spatial resolution consistent with the input GSV map used in this study is not yet available. For this reason, the distribution of forest categories was derived from the Corine Land Cover (CLC) maps, which are available for the reference years

2006, 2012, and 2018. In Italy, CLC is the only spatial source that provides consistent information on forest category distribution across different years on a national scale. The CLC project was started in 1990 by the European Environmental Agency (Büttner et al., 2004) and consists of a European-scale land-use monitoring program with a 44-class nomenclature system produced by photointerpretation of high-resolution satellite imagery. CLC uses a minimum mapping unit (MMU) of 25 ha and a minimum mapping width (MMW) of 100 m (EEA, 2007). The original CLC nomenclature system classifies the forest into three classes: broadleaves, coniferous, and mixed forests. In the Italian implementation the CLC maps produced by the *Istituto Superiore per la Protezione e la Ricerca Ambientale* (ISPRA) classify forests into 28 classes (Bologna et al., 2004). In this study, we re-classified forests into 18 classes (Annex I). Forest category maps were obtained from the original CLC vector products by rasterizing at the same spatial resolution as the baseline GSV map. Then we masked out the non-forest categories by assigning them to the ‘non-forest’ class.

Our spatial approach requires for each year a newly updated forest category map. Since the CLC project is not updated yearly, we used the forest category map of 2006 for the years 2005–2009, that of 2012 for 2010–2014, and that of 2018 for 2015–2018 (Fig. 2). This procedure was considered appropriate since the percentual change of forest area

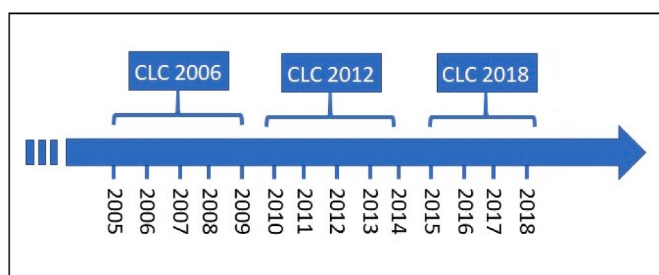


Fig. 2. Corine Land Cover (CLC) forest category maps used for each year of the study period.

based on the CLC maps is limited. In the period 2006–2012, considering both increments and decrements, the forest area changed only by 741 km² (the 0.74% of the forest area) while in the period 2012–2018, it changed only by 705 km² (the 0.70% of the forest area).

2.4. National collection of yield tables

The national collection of yield tables from Federici et al. (2001) was used to model the current increment of forests as a function of GSV and the GSV as a function of forest age. Yield tables reported the GSV and current increment as a function of forest age for 27 species within 13 genera. The 27 species were linked to the 18 forest categories derived from CLC (see section 2.3), with *ad-hoc* harmonization bridges developed for this study. Bridges preserve data attributes based on different definitions, allowing their comparison at a higher hierarchical level (Annex I).

2.5. Forest disturbances time-series maps

Data on the spatial distribution of forest disturbances in the period 2004–2018 were needed to account for forest harvesting and other disturbances in GSV and the carbon stock estimation process. These data were produced with the 3I3D algorithm (Francini et al., 2021) recently implemented in Google Earth Engine (GEE) (Francini et al., 2022b), a cloud-based platform that can process massive amounts of remotely sensed data (Gorelick et al., 2017).

3I3D is an unsupervised algorithm that predicts forest disturbances requiring no input parameters or calibration. It analyses the pattern over three sequential years of three indexes (3I) of photosynthetic activity used as three-dimensional (3D) space axes. 3I3D was applied using yearly cloud-free composites of Landsat surface reflectance images atmospherically corrected with LEDAPS (Wolfe et al., 2004) and acquired with a solar zenith angle smaller than 76°. Candidate images were acquired during the vegetative season (between Jun and Aug), with a cloud cover lower than 50% in the scene. As a result, we obtained a collection of about 800 images per year. We excluded those pixels covered by clouds, shadows, water, and snow (Foga et al., 2017) and pixels with an opacity value greater than 0.3. For each year, we then selected the “best” pixels among the remaining ones using the Best Available Pixel procedure (BAP) (Griffiths et al., 2013; White et al., 2016), obtaining a BAP-collection of cloud-free composite for each year between 2004 and 2018. Specifically, the BAP pixel selection is based on a set of scores, among which i) the sensor, ii) the day of the year, iii) the distance to cloud or cloud shadows, and iv) the opacity. The BAP was recently implemented in GEE, with the full code openly available. A detailed description of the application, guidance, and suggestions on BAP parameters setting is provided on GitHub (https://code.earthengine.google.com/?accept_repo=users/sfrancini/bap).

We used BAP cloud-free composites as input for the 3I3D algorithm to predict forest disturbances with a MMU of 500 m² over the study period. Official forest data on burned areas, annually produced and released for the same period by the Italian Forest Service (Comando Unità Forestali, Ambientali e Agroalimentari di Carabinieri), have been also used. This dataset includes burnt areas from forest fires acquired through a ground survey with the Global Navigation Satellite System (GNSS).

We merged the official national database of forest fires with the forest disturbances map produced by 3I3D (with an OR logical operator), classifying forest pixels for each investigated year in “disturbed” or “undisturbed”. Based on these maps, we finally produced the “age” of disturbed forests for each investigated year as the number of years since the last disturbance event (YSLD).

2.6. Calibration data

To optimize and calibrate the procedure, we used 9258 circular plots

where the GSV was measured in the field between 2006 and 2019 in the framework of local forest inventories (Fig. 1). The plots are distributed under different environmental conditions and forest categories over the whole country. The same survey protocol of the Italian NFI was adopted in all these plots. The tree-level GSV was determined by the allometric models used for the Italian NFI (Tabacchi et al., 2011), and then tree-level data were aggregated at the plot level. For this study, allometric model prediction and GNSS position uncertainties are expected to be negligible for the spatial resolution adopted (McRoberts et al., 2013, 2016, 2018; Chirici et al., 2020). The mean GSV in this calibration dataset is 216 m³ ha⁻¹, with a maximum of 1482.4 and a standard deviation of 155 m³ ha⁻¹. To find the most appropriate solution, we evaluated the models in terms of RMSE% at the plot level, comparing GSV estimates with the observed one.

2.7. Validation data

To validate the results, we compared aggregated regional GSV and carbon stock estimates for 2015 based on the pixel level values we produced (the GSV₂₀₁₅ 23 m resolution map) with official regional estimates from the Italian NFI. We also compared aggregated values of GSV and carbon stock produced by our method with the official estimates reported in the Italian 2006–2019 GHG inventory. Just as in the calibration, we compared the accuracy of our results in terms of RMSE%, calculated as the percent of RMSE against the mean official values.

3. Methods

3.1. Overview of the spatial approach

For the years not covered by the periodic Italian NFI, our spatial approach for predicting GSV and carbon stocks was carried out differently for pixels belonging to disturbed and undisturbed forests. Annual stock changes were predicted for each 23 m pixel, using the GSV₂₀₀₅ mapped for 2005 and the YSLD as unique drivers. The GSV₂₀₀₅ was selected since it is strictly related to the above-ground biomass and carbon stock, and it is directly measured by the NFI in the field. While the YSLD was selected because it can be easily obtained based on change detection algorithms, such as the 3I3D, and it is the primary driver of forest variables in yield tables.

Our approach uses the first derivative of the Richards function (Eq. (1)) to calculate the current increment (Eq. (2)) as a function of the GSV in undisturbed forests for each of the 18 CLC forest categories (Federici et al., 2008). The following equation defines the Richards function:

$$\frac{dy}{dt} = \frac{k}{v} \bullet y \left[1 - \left(\frac{y}{a} \right)^v \right] + y_0 \text{ first derivative} \quad (1)$$

Its analytical solution defines the Richards growth curve:

$$y = a \bullet \left[1 - e^{(\beta - kt)} \right]^{-\frac{1}{v}} \quad (2)$$

where the general constraints for the parameters are $a, k > 0$; $-1 \leq \beta \leq \infty$; $v \neq 0$.

The curve is bounded and monotonic, highly flexible thanks to its four parameters. It can be efficiently approximated to a logistic ($a \rightarrow \infty$, $v > 0$), exponential ($v > 1$), or other most used growth curves. However, due to the number of parameters and their high covariance, the curve is difficult to fit and can cause problems during the non-linear regression (Federici et al., 2008). The current increment represents the dependent variable, while the independent variable is the GSV map.

In disturbed forest areas, different potential models were evaluated for estimating GSV as a function of YSLD for each forest category. Using the data in the yield tables collection, we tested four regression models, two non-parametric, random forests and Support Vector Machine (SVM), and two parametric, polynomial, and linear regression. The GSV represents the dependent variable, while the independent variable is the

forest age from yield tables.

The optimization was fine-tuned by picking the most accurate model based on the correlation coefficient (r^2). All four regression models yielded comparable results with only slight differences. The SVM model slightly outperformed other approaches, with an average r^2 among the forest categories of 0.91, against 0.90 of random forests and 0.88 of polynomial and linear regression.

After the model fitting for each category in undisturbed and disturbed forest areas, the above-ground carbon stock is predicted in the five steps described below:

1. Starting from the initial GSV₂₀₀₅ map, the current increment is estimated via the Richards function in undisturbed forest areas for each year and for each forest category, based on the relationships between GSV and current increment derived from yield tables.
2. Similar to point 1, GSV in disturbed forest areas is estimated for each year, and forest category with the corresponding SVM model, based on the relationships between YSLD and GSV derived from the yield tables.
3. For each year and forest category, the GSV is calculated as the sum of the previous year's GSV and the estimated current increment, subtracting the losses due to natural mortality and adding the GSV in disturbed forest areas calculated in step 2.
4. For each year and forest category, the GSV ($\text{m}^3 \text{ha}^{-1}$) is converted in above-ground biomass (AGB) (Mg d.m. ha^{-1}) with the equation:

$$\text{AGB} = \text{GSV} * \text{BEF} * \text{WBD} \quad (3)$$

where GSV is the growing stock volume calculated in step 3, BEF is the category-specific biomass expansion factor (dimensionless), and WBD is the wood basal density (Mg d.m. m^{-3}).

5. Carbon stocks are derived from AGB by applying the default carbon fraction factor of 0.47 (IPCC et al., 2006).

Following the IPCC Good Practice Guidance for LULUCF (IPCC et al., 2006), the average rate of natural mortality was set equal to 0.116% for evergreen categories, 0.117% for deciduous categories, and 0.1165% for mixed categories, while BEF and WBD are those applied by the *For-est* model (Federici et al., 2008).

The detailed methodology is described here below.

3.2. GSV estimation in undisturbed forests

In undisturbed forests, the GSV for the year n was computed at pixel level by adding the current increment of the year $n-1$ to the GSV of the year $n-1$ and subtracting losses due to natural mortality. We used an age-independent model to create annual maps of the current increment. Category-specific growth models were constructed using the data of the national yield tables collection to calculate the current increment ($\text{m}^3 \text{ha}^{-1} \text{y}^{-1}$) as a function of GSV ($\text{m}^3 \text{ha}^{-1}$), using the first derivative of the Richards function (eq. (1)). The GSV represents the independent variable x , while the dependent variable y is the correspondent current increment. The forest category-specific Richards functions were fitted using all the fertility classes of the yield tables. The parameterization was based on a 25 iterations-bootstrap-cross-validation procedure. For each bootstrap iteration and species, the RMSE was calculated, and the model which reported the lowest RMSE was chosen as the final model. RMSE was calculated as:

$$\text{RMSE}_{sp} = \sqrt{\frac{\sum_{i=1}^n (y_i - \hat{y}_i)^2}{n}} \quad (4)$$

where n is the number of observations in the yield tables for the species sp , y_i is the current increment value reported in the yields table for the i -th observation and \hat{y}_i is the current increment predicted from the model

for the i -th observation.

We started the process based on the GSV₂₀₀₅ map produced by Vangi et al. (2021), and we produced the updated GSV₂₀₀₆ map applying, for each 23×23 m undisturbed forest pixel, the current increment per hectare predicted for each forest category with the corresponding growth curves and subtracting the natural mortality. Then, the process was repeated for 2007 based on GSV₂₀₀₆ and so on until 2018.

By applying the Richard first derivative approach, the current increment was estimated with an average RMSE (as per eq. (4)) of 49.4% across all forest categories, with significant variations among forest categories, mainly due to the number of observations and fertility classes available in the yield tables. Some of the most frequent forest categories in Italy obtained the best results, such as the maple-ash-hornbeam mixed forests (RMSE = 22%), the Mediterranean maquis (RMSE = 13%), and the chestnut forests (RMSE = 26%), which altogether represent more than 25% of the national forest area.

The best results were obtained by the exotic plantations category with an RMSE of 3.2%, most probably because of their homogeneous growth behaviour. In comparison, the mixed conifers category obtained the worst result with an RMSE of 95% (but they cover only 4.4% of the forest area), most probably because of their heterogeneous composition.

3.3. GSV estimation in disturbed forests

We already know that forest age is not an appropriate predictor for estimating the productivity of undisturbed forests in Italy since they are mainly uneven-aged and are characterized by a complex mosaic of different ages or cohorts (Federici et al., 2008; Frate et al., 2015). Instead, in most disturbed forests, trees regrowing after the disturbance results in even-aged stands, at least for the first years after the disturbance. This is particularly true for clearcuts in coppice forest (Chirici et al., 2020), which represent the most common forest disturbance in Italy, based on Francini et al. (2022, a), representing 80% of all forest loggings in Italy. In such a situation, forest age can be used to predict GSV growth in disturbed stands using the data in the national yields table collection. We used forest categories-specific SVM models to predict the GSV based on forest age with a radial basis kernel function. SVM approaches are known to be robust against outliers and overfitting and are well-suited for approaching problems with a limited amount of training data. These algorithms can generate non-linear decision surfaces by mapping the data into a high-dimensional space through non-linear mapping functions called kernel functions (Cortes and Vapnik, 1995; Pal and Mather, 2005), allowing the separation of the data through linear hyperplanes (Dixon and Candade, 2008). Among the kernel functions, one of the most used is the radial basis function, which has two tuning parameters C (regularization parameter) and γ (kernel width) (Kavzoglu and Colkesen, 2009). An in-depth explanation of SVM-based models and kernels is presented in Smola and Schölkopf (2004) and Kavzoglu and Colkesen (2009). Implementations of SVM models in RS can be found in Mountrakis et al. (2011). In this study, the parameters of SVM and radial kernel (C , γ) were determined by bootstrap cross-validation with 25 iterations using the grid search method, by selecting the pairs of parameters that produce the lowest cross-validation RMSE among an exponentially growing sequence of the parameters ($C = 2^{1/2}, 2^1, \dots, 2^5; \gamma = 2^{-5}, 2^{-4}, \dots, 2^0$). For each bootstrap iteration and species, the RMSE was calculated as per eq. (4), and the model which obtained the lowest RMSE was chosen as the final model.

In disturbed areas identified by the 3I3D algorithm, the GSV was computed for each year and forest category by applying the category-specific SVM models fitted from the yield tables data. The YSLD for the year n was used as the independent variable to predict the GSV _{n} in each disturbed pixel, obtaining a GSV map of forest disturbances for each year between 2005 and 2018.

The complete GSV _{n} map was produced by overlaying the GSV _{n} maps of disturbed and undisturbed forests.

The SVM models led to an average RMSE of 35.9%, with a maximum

of 64% for the mixed forests with the prevalence of coniferous and a minimum of 5% for the maple-ash-hornbeam mixed forest. As for the Richard models, we observed significant variations depending on the number of fertility classes in yield tables.

3.4. Carbon stock conversion

Once estimated the GSV, amounts of AGB are consequently assessed. For every forest typology, starting from the GSV, the AGB (Mg d.m. ha^{-1}) is calculated, through equation (3), following the approach presented in Federici et al. (2008).

Carbon stock maps were derived from AGB maps by applying the default factor for carbon fractions of 0.47 (IPCC et al., 2006).

The pixel-level predictions of GSV and stocked carbon were aggregated at the regional level for each year.

4. Results

4.1. GSV and carbon stock estimation

The spatial approach for estimating annual GSV and above-ground carbon pool was applied to produce 23 m resolution yearly pixel-level estimates from 2005 to 2018. Based on our results, the GSV increased in Italy by 522 million m^3 moving from an average of $130 \text{ m}^3 \text{ ha}^{-1}$ to $180 \text{ m}^3 \text{ ha}^{-1}$. GSV and above-ground carbon stocks time series are reported in Annex II. Carbon stock increased by 206 million of t in the same period, moving from $36.9 \text{ Mg C ha}^{-1}$ to $59.3 \text{ Mg C ha}^{-1}$, with an average accumulation rate of $14.7 \text{ mln Mg C y}^{-1}$. Regionally, most of the GSV and carbon gains dominate mountain landscapes of the Alps and Apennines mountains. In the years 2005–2018, among all forest categories, beech forests accumulated the most GSV, with about 3926 mln of m^3 corresponding to 54 mln Mg C of above-ground carbon stored (about 28.3% of the total carbon absorbed by national forests), followed by mixed broadleaf forests (34 mln Mg C, about 18% of the total) and the fir/spruce forests (23 mln Mg C, 12% of the total). Regardless of the forest category, in the study period, carbon accumulation is reflected mainly in the increase of the carbon density rather than the increase of the total forest area, which amounts to 145,000 ha according to the CLC maps.

Northern regions (Trentino-Alto Adige, Piemonte, Lombardia, Veneto, Friuli Venezia Giulia) have the highest GSV accumulation in terms of absolute and per hectare figures, accounting for 54% of the national total. Other regions with significant GSV accumulation are Toscana, Sardegna, and Emilia-Romagna, contributing 20% to the national GSV growth (each up to 20 mln m^3 in the study period). In contrast, most southern regions (Molise, Campania, Puglia, Basilicata, Sicilia) show the least accumulation of GSV, less than 8 mln m^3 between 2005 and 2018. Carbon uptake has similar patterns, exhibiting higher absolute and per

hectare storage in many northern regions (Trentino-Alto Adige, Piemonte, Lombardia, Veneto) and lower in the southern ones (Molise, Puglia, Umbria) (Fig. 4). Also, at the regional level, the accumulation of GSV and carbon stock is primarily driven by the increase of GSV and carbon density rather than the total forest area. This is probably due to a decrease in the harvested area over the last two decades, which allowed for significant growth in GSV per unit area (Francini et al., 2022a; b).

In Fig. 3 is reported the overall absolute accumulation of GSV and carbon stock at the regional level over the study period.

4.2. Validation and comparison of our results

During the optimization phase the 23 m resolution pixel level estimations of GSV estimates obtained applying the best configuration of our models where compared against the GSV measured in the field in 9258 independent plots acquired in different years in the period 2006–2018. From such comparison the average RMSE% was 57% ranging between 89.6% in 2009 and 34% in 2015, (Fig. 5). The bias across years was $-3.7 \text{ m}^3 \text{ ha}^{-1}$, with the minimum in 2010 ($-0.2 \text{ m}^3 \text{ ha}^{-1}$) and the maximum in 2013 and 2015 (-70.3 and $-60.2 \text{ m}^3 \text{ ha}^{-1}$). These values are in the range of previous experiences (Immitzer et al., 2016; Chirici et al., 2020; Vangi et al., 2021).

Pixel level estimations for the year 2015 where aggregated for administrative Regions and compared with the official 2015 NFI estimates (INFC, 2021), resulting in a 6.2% and 1.1% difference at the national level for GSV and carbon stock, respectively (calculated as the mean value of the difference between predicted and observed results). We obtained an RMSE of 19.5% and 17.8% at the regional level and an r^2 of 0.94 and 0.92 for GSV and carbon stock, respectively (Fig. 6). RMSE was calculated as:

$$RMSE_{NFI} = \sqrt{\frac{\sum_{i=1}^n (y_{NFI_i} - \hat{y}_i)^2}{n_{rg}}} \quad (5)$$

where n_{rg} is the number of Italian regions, y_{NFI_i} is the official NFI value (of GSV and carbon stock) for the i -th region and \hat{y}_i is the aggregated estimation (of GSV and carbon stock) produced by the spatial approach for the i -th region.

The data for the comparison against the 3rd Italian NFI (INFC, 2021) are presented in Annex III.

Finally, following the same procedure, our GSV predictions aggregated for Italian Regions were compared with official estimates of Italian GHG inventories for 2005–2018, obtaining an overall RMSE% of 28.6% and an r^2 of 0.77 with a growing trend over time. Here the RMSE was calculated as:

$$RMSE_{GHG} = \sqrt{\frac{\sum_{i=1}^n (y_{GHG_i} - \hat{y}_i)^2}{n_{rg}}} \quad (6)$$

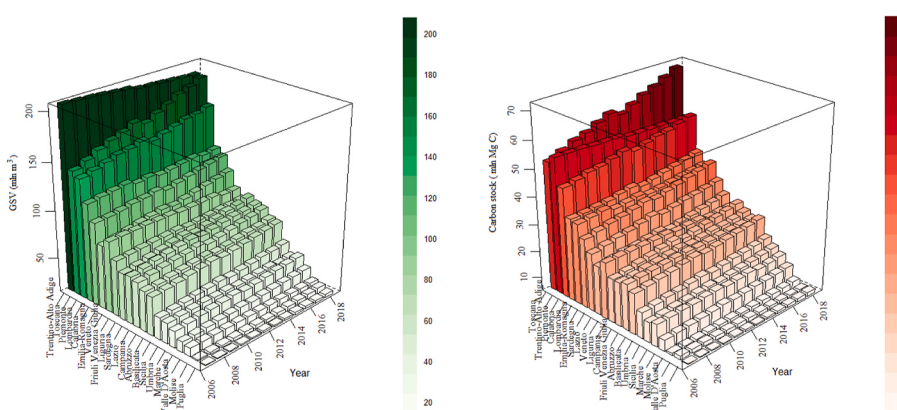


Fig. 3. Annual GSV (left) and carbon stock (right) at the regional level from 2005 to 2018.

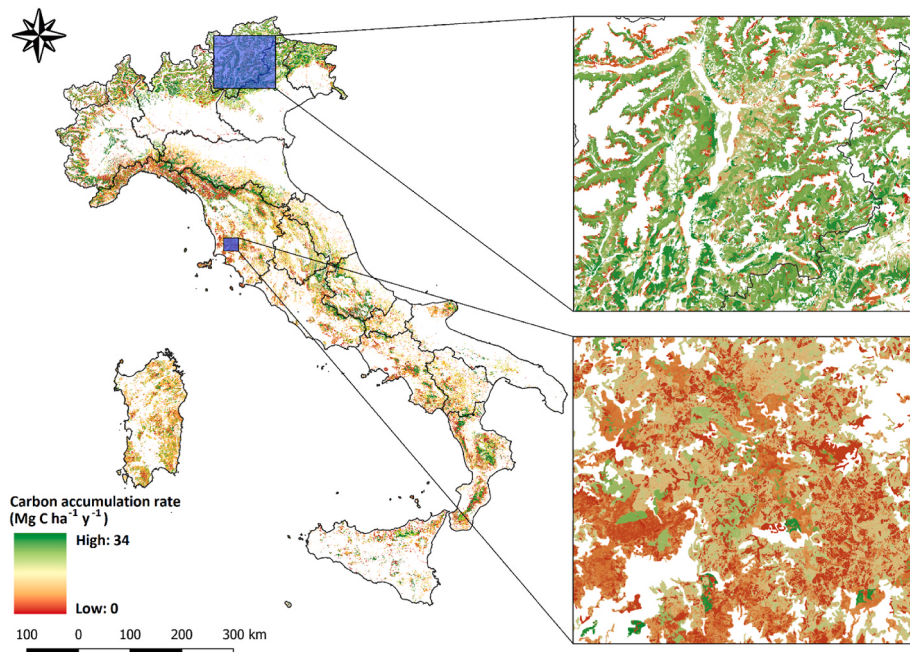


Fig. 4. Left: Pixel-level carbon accumulation rate in forests ($\text{Mg C ha}^{-1} \text{y}^{-1}$) for 2005–2018.

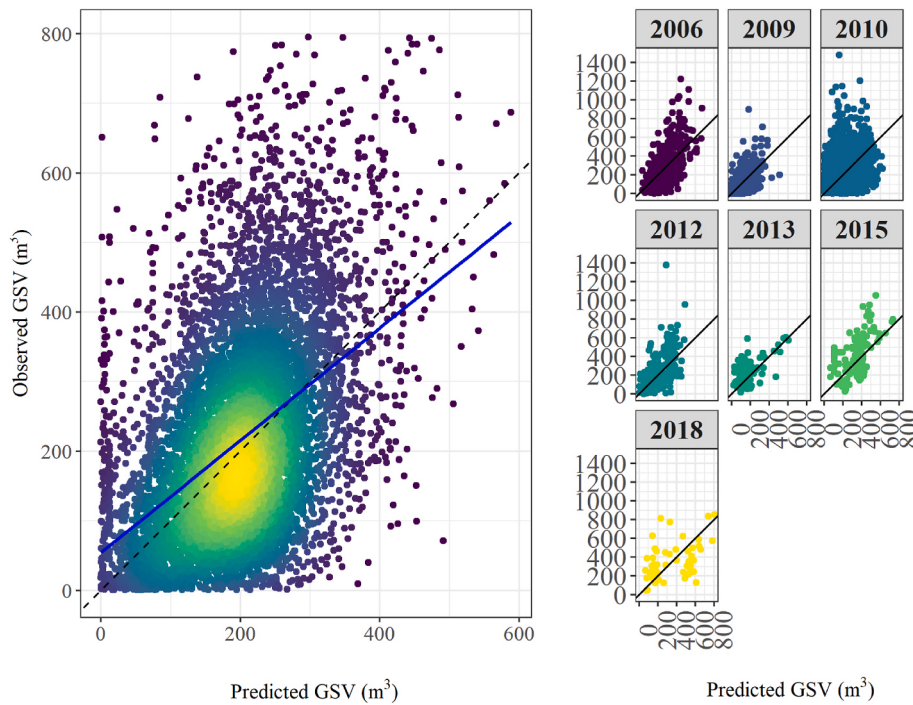


Fig. 5. Left: observed GSV in the field plot against predicted GSV; Right: observed against predicted GSV for each year. Blue is the regression line.

where n_{rg} is the number of Italian regions, y_{GHG_i} is the official GHG inventory value (of GSV and carbon stock) for the i -th region and \hat{y}_i is the aggregated estimation (of GSV and carbon stock) produced by the spatial approach for the i -th region.

The carbon stock was also compared against the official Italian GHG inventory (LULUCF sector, forest land remaining forest land category) for the same period (ISPRRA, 2021a; b), yielding an r^2 of 0.88 and an overall RMSE% (as per equation (6)) of 23.1% and 17.2% among years and regions, respectively. As for the GSV, consistency with official estimates has worsened over the years, while at the regional level reached

the minimum in Piemonte (RMSE 2.5%) and the maximum in Trentino-Alto Adige (RMSE 48.6%). Thirteen out of 20 regions showed an RMSE% less than 15%, with seven regions less than 10%. Fig. 7 reports the regional comparison between our results and the official estimates from the national GHG inventory (ISPRRA, 2021b; b) regarding GSV and carbon stock.

5. Discussion

The main objective of the study was to develop a new spatial

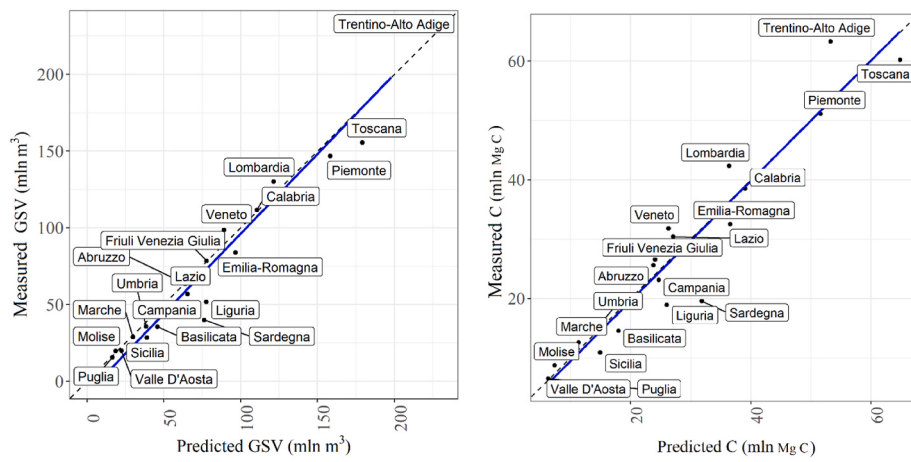


Fig. 6. Left: INFC 2015 GSV against predicted GSV; Right: INFC 2015 carbon stock against predicted carbon stock. The dotted line is the $y = x$ line, and the blue is the regression line.

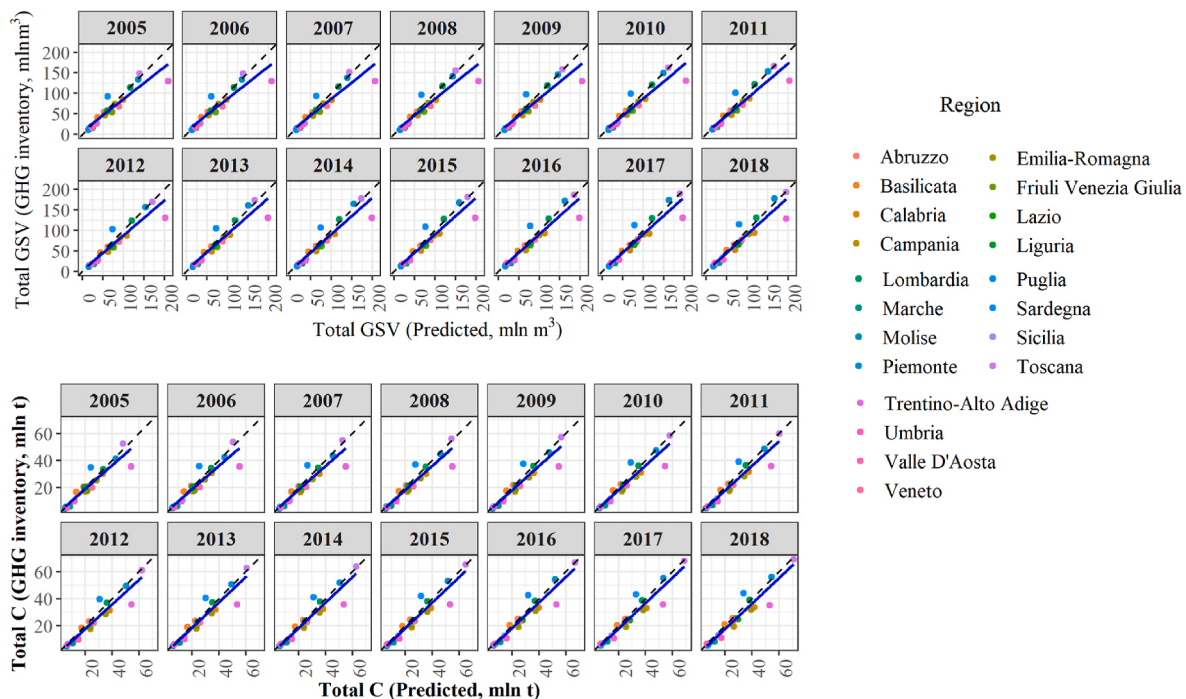


Fig. 7. Comparison of GSV (right) and carbon stock (left) at the regional level against the Italian GHG inventory LULUCF sector, forest land remaining forest land category) for each year of the study period.

approach for producing wall-to-wall high-resolution yearly GSV and carbon stock predictions between consecutive NFI field measurements, exploiting remotely sensed and auxiliary data, which could be used for operational application and to respond to international reporting tasks. Empirical models developed by interpolating data from NFI field plots could produce updated estimates only for short-term predictions, for which growth conditions such as climate and management regimes are expected to be stable (Peng, 2000). Moreover, in such models, stand variables are driven by the age of the forest, but in natural conditions, growth is strictly related to species and local environmental conditions. For these reasons, our novel approach for estimating carbon stocks and changes at the national and regional level in the above-ground carbon pool is driven only by NFI GSV data and yield models.

The yearly wall-to-wall maps of GSV and carbon stock can support reporting activities and forest management at any scale by aggregating pixel-level predictions producing small-area estimations, for example,

using the estimators proposed by Chirici et al. (2020).

Our results agreed with those reported by the official Italian GHG inventory and show an increasing trend in the above-ground carbon pool that reflects both the expansion of forest areas (according to NFI, in the period 2005–2015, forest areas increased by 58,692 ha y^{-1} , approximatively 0.5% of total forest area in 2015) and the increased growing stock resulting from a forest harvest rate lower than the current increment. The organic carbon in the above-ground biomass of the Italian forest exceeded 566 million Mg C in 2018, with a different contribution of regions and forest categories in terms of fixed organic carbon. GSV and carbon stock distribution among forest categories comply with the 2020 Italian FAO FRA report for 2005 and 2010, with beech and spruce/fir forests accounting for 40% and 36% of the total GSV and carbon stock, respectively. Due to their limited area nationwide, the forest categories contributing the least to carbon storage (less than 0.5% of the total) are exotic conifers, broadleaf plantations, wood

arboriculture, and riparian formations. It is worth noting that other wooded vegetation in open and shrublands has a relatively significant contribution to terrestrial carbon sinks, storing more than seven mln of Mg C of carbon (approximately 5% of the national total).

Large forest areas characterize regions with the most GSV and carbon stock and highly carbon-storing forest categories (beech, mixed broadleaf, fir/spruce, larch, Mediterranean pines, exotic plantations), despite most of these categories are subject to intense forest harvesting, as resulted from 3I3D disturbances maps. In this regard, it is worth noting that the major disagreement between our approach and the official ISPRA estimates is found in the northern regions and particularly in Trentino-Alto Adige, which leads to the maximum relative RMSE (for which the GHG inventories estimate a decrease in GSV and carbon stock over the study period). This mismatch is primarily due to underestimating the number of forest disturbances, especially in high-forest stands of the main mountain ranges, where silvicultural treatments are based on continuous canopy cover approaches that are difficult to detect by optical satellite imagery. The lack of fire data compounds the underestimation of disturbances before 2007 and after 2017.

Moreover, for the Autonomous Provinces of Trento and Bolzano, the database of forest fires includes only fires greater than 20 ha, potentially increasing the underestimation of the total number of disturbances. Without offsetting for forest harvests and forest fires, the GSV builds up rapidly, driven by the increase of the current increment of highly productive forest categories, leading to significant overestimates and large values of RMSE. However, in Trentino-Alto Adige, the mismatch between our results and the 2015 NFI is less evident, with an underestimation of only 13% and 15% for GSV and carbon stock, respectively.

Another source of uncertainty is the overestimation of the current increment with the Richard first derivative compared to the 2nd NFI field measurement. This finding contrasts with the underestimation reported by Federici et al. (2008) compared to the 1st NFI data. The discrepancy between the predicted and reported current increment of NFI is likely driven by three factors: i) an outdated collection of national yield tables which no longer reflect the country's real average quality of forest sites; ii) Richard's first derivatives were fitted against all species quality class data in yield tables, and since species data were aggregated to match the species composition of each forest category as closely as possible, the predicted current increment of less productive species can be overestimated, especially for mixed forest categories; iii) the overestimation of the GSV in the initial 2005 GSV map, used as the independent variable for Richards functions. This evidence was reported by Vangi et al. (2021). SVM models generally performed better than the Richards function for the same forest categories, except for chestnut, hygrophilous formations, exotic broadleaf plantations, larch, and stone pine categories. For those forest categories, the SVM model underestimates GSV for older age classes, for instance, over ten years for exotic broadleaf plantations and riparian formations, 25 years for chestnut, and more than 80 years for the remaining forest categories. Hence, the effect of underestimation only affects categories of hygrophilous formations and non-native species plantations, as the years since the last disturbance can be at most equal to 13 years (2018–2005).

During the optimization phase using the dataset of independent field plots the differences between pixel-level measured and estimated GSV increased over time. This bias with under-predictions for plots with high values of GSV, especially for years 2009, 2012, and 2015, can be caused by the well-known saturation effect, especially in dense crown cover and steep terrain (Nilsson et al., 2017; Giannetti et al., 2018; Chirici et al., 2020). Such dataset was acquired for those years in forests managed for productive purposes or, more in general, with an average GSV much greater ($420 \text{ m}^3 \text{ ha}^{-1}$) than those measured in INFC plots ($140 \text{ m}^3 \text{ ha}^{-1}$). In this phase the largest bias was observed in southern regions and in the islands, that are characterized by sparse Mediterranean vegetation where modeling the GSV resulted more difficult in previous experiences too (D'Amico et al., 2021; Vangi et al., 2021). But it is important to note that wall-to-wall spatial predictions from NFI field observations should

never be used at the pixel level since the single pixel predictions may be affected by a consistent bias (McRoberts and Tomppo, 2007).

However, when we aggregated the pixel level estimations at the regional level, we obtained very satisfying results consistent both with the Italian GHG inventory and the 3rd NFI (INFC, 2021). It is worth noting that, concerning the 3rd NFI in 2015, the carbon stock difference at the regional level was minor than the GSV difference (Fig. 7). This is interesting because it proves that the species-specific BEF and WBD together with the spatial distribution of forest categories can compensate for the overestimation of GSV. Under this point of view, our estimates are conservative since the approach neither overestimates increases nor underestimates decreases in carbon stocks with respect to the NFI official estimations.

As soon as new high-resolution forest types maps will be available, the use of the CLC maps should be reconsidered. Several studies have already highlighted the limitations of CLC maps in forestry, primarily because of the wide MMU of 25 ha (Seebach et al., 2012; Vizzari et al., 2015; Vangi et al., 2021).

6. Conclusions

To the best of our knowledge, this is the first study to provide yearly high-resolution GSV, AGB, and carbon stock wall-to-wall time-series maps for the whole national territory in Italy, allowing an in-depth analysis of the forest carbon stock changes, consistently with the IPCC guidelines. The spatial nature of our results enables small-scale estimates by aggregating individual pixel predictions, enhancing the spatial resolution of traditional NFI design-based estimates (Chirici et al., 2020), and can be embedded into decision support systems to support sustainable forest management and precision forestry activities. Furthermore, the knowledge of the spatial distribution of carbon among forest categories can be of fundamental importance under the climate mitigation goals of the Paris Agreement (UNFCCC, 2015).

The growing need for new information and technological advances is driving the rapid evolution of forest monitoring and assessment. However, the exploitation of the latter and their implementation within international reporting processes should be evidence-based (Corona, 2018).

This study provides an innovative spatial framework to track GSV and carbon stock changes between NFI surveys at local to national scales, providing a reliable monitoring approach to meet the increasing interests of non-government and private entities in carbon offset investments. Our new method incorporates forest disturbance between surveys, such as forest fires and harvesting, thanks to Landsat-based time-series metrics exploited by the 3I3D unsupervised change detection algorithm, which has already proved to be a better solution in the Mediterranean environment than previous algorithms (Francini et al., 2021). The 3I3D algorithm here demonstrated to be a valid solution for deriving forest age to track the GSV regrowth after disturbances by applying age-dependent relationships in yield tables.

The approach could be improved with 2015 NFI data, as well as updated information on allometric models and yield tables, allowing better model calibration and quality assurance routines. It is worth remembering that although GHG inventories are not measured on the ground, they represent official data sources used for national and international reporting activities.

Nevertheless, the availability of ground-based carbon content data to calibrate and validate the method is desirable. For this reason, as soon as they will be available 2015 NFI carbon stock ground data will allow the evaluation of the pixel-level performance for the carbon stock map for 2015, providing insight into the method's effectiveness. The availability of an official high-resolution national forest map and wall-to-wall multitemporal ALS data could also be fundamental for improving the quality of GSV and carbon stock spatial estimations.

Author's contributions

Conceptualization, G.C., E.V., and G.D.; methodology, E.V., G.D., S.F.; software, E.V.; validation, E.V.; formal analysis, E.V., G.D.; investigation, E.V., G.D.; data curation, E.V., G.D.; writing—original draft preparation, E.V. All authors have contributed to the drafting of the manuscript. All the authors assisted in the quality control, and revisions of the manuscript.

Declaration of competing interest

The authors declare that they have no known competing financial interests or personal relationships that could have appeared to influence the work reported in this paper.

Data availability

Data will be made available on request.

Acknowledgements

This study was partially supported by the following projects:

MULTIFOR “Multi-scale observations to predict Forest response to pollution and climate change” PRIN 2020 Research Project of National Relevance funded by the Italian Ministry of University and Research (prot. 2020E52THS);

SUPERB “Systemic solutions for upscaling of urgent ecosystem restoration for forest related biodiversity and ecosystem services” H2020 project funded by the European Commission, number 101036849 call LC-GD-7-1-2020;

EFINET “European Forest Information Network” funded by the European Forest Institute, Network Fund G-01-2021.

Appendix A. Supplementary data

Supplementary data to this article can be found online at <https://doi.org/10.1016/j.envsoft.2022.105580>.

References

- Bologna, S., Chirici, G., Corona, P., Marchetti, M., Pugliese, A., Munafò, M., 2004. Sviluppo e implementazione del IV livello Corine Land Cover per i territori boscati e ambienti semi-naturali in Italia. Paper presented at the annual meeting for the Society of ASITA, pp. 467–472.
- Büttner, G., Feranec, J., Jaffrain, G., Mari, L., Maucha, G., Soukup, T., 2004. The Corine Land Cover 2000 Project. EARSeL eProceedings 3, 3/2004 331. Available online. <http://citeseerx.ist.psu.edu/viewdoc/download?doi=10.1.1.618.9940&rep=rep1&type=pdf>
- Chirici, G., Giannetti, F., McRoberts, R.E., Travaglini, D., Pecchi, M., Maselli, F., Chiesi, M., Corona, P., 2020. Wall-to-wall spatial prediction of growing stock volume based on Italian National Forest Inventory plots and remotely sensed data. Int. J. Appl. Earth Obs. Geoinf. 84, 101959. <https://doi.org/10.1016/J.JAG.2019.101959>
- Condés, S., McRoberts, R.E., 2017. Updating national forest inventory estimates of growing stock volume using hybrid inference. For. Ecol. Manag. 400, 48–57. <https://doi.org/10.1016/j.foreco.2017.04.046>
- Corona, P., 2010. Integration of forest mapping and inventory to support forest management. iFor. Biogeosci. For. 3, 59–64. <https://doi.org/10.3832/ifor0531-003>
- Corona, P., 2018. Communicating facts, findings and thinking to support evidence-based strategies and decisions. Annals of Silvicultural Research 42, 1–2. <https://doi.org/10.12899/ASR-1617>
- Cortes, C., Vapnik, V., 1995. Support-vector networks. Mach. Learn. 20 (3), 273–297.
- Dalponte, M., Coomes, D.A., 2016. Tree-centric mapping of forest carbon density from airborne laser scanning and hyperspectral data. Methods Ecol. Evol. 7 (10), 1236–1245. <https://doi.org/10.1111/2041-210X.12575>.
- Di Cosmo, L., Gasparini, P., Tabacchi, G., 2016. A national-scale, stand-level model to predict total above-ground tree biomass from growing stock volume. For. Ecol. Manag. 361, 269–276. <https://doi.org/10.1016/j.foreco.2015.11.008>, 0378–1127.
- Dixon, B., Candade, N., 2008. Multispectral landuse classification using neural networks and support vector machines: one or the other, or both? Int. J. Rem. Sens. 29 (4), 1185–1206. <https://doi.org/10.1080/01431160701294661>.
- D’Amico, G., Vangi, E., Francini, S., Giannetti, F., Nicolaci, A., Travaglini, D., Massai, L., Giambastiani, Y., Terranova, C., Chirici, G., 2021. Are we ready for a National Forest Information System? State of the art of forest maps and airborne laser scanning data availability in Italy. iForest 14, 144–154. <https://doi.org/10.3832/ifor3648-014>
- EEA, 2007. European Environmental Agency, environmental statement 2007. Office for Official Publications of the European Communities, Luxembourg, pp. 1–14. ISBN 978-92-9167-936-2.
- Federici, S., Quarantino, R., Papale, D., Tulipano, S., Valentini, R., 2001. Sistema Informatico Delle Tavole Alsometriche d’Italia, DiSAFRI – Università Degli Studi Della Tuscia [online] URL: <http://gaia.agraria.unitus.it>.
- Federici, S., Vitullo, M., Tulipano, S., De Lauretis, R., Seufert, G., 2008. An approach to estimate carbon stocks changes in forest carbon pools under the UNFCCC: the Italian case. iForest 1, 86–95 [online: 2008-05-19] URL: <http://www.sisef.it/iforest/>.
- Foga, S., Scaramuzza, P.L., Guo, S., Zhu, Z., Dilley, R.D., Beckmann, T., Schmidt, G.L., Dwyer, J.L., Hughes, M.J., Laue, B., 2017. Cloud detection algorithm comparison and validation for operational Landsat data products. Rem. Sens. Environ. 194, 379–390. <https://doi.org/10.1016/j.rse.2017.03.026>
- Francini, S., McRoberts, Ronald E., Giannetti, F., Marchetti, M., Mugnozza, G.S., Chirici, G., 2021. The Three Indices Three Dimensions (3ID3) algorithm: a new method for forest disturbance mapping and area estimation based on optical remotely sensed imagery. Int. J. Rem. Sens. 42 (12), 4693–4711. <https://doi.org/10.1080/01431161.2021.1899334>
- Francini, S., McRoberts, Ronald E., D’Amico, G., Coops, N.C., Hermosilla, T., White, J.C., Wulder, M.A., et al., 2022a. An open science and open data approach for the statistically robust estimation of forest disturbance areas. Int. J. Appl. Earth Obs. Geoinf. 106, 102663. <https://doi.org/10.1016/j.jag.2021.102663>
- Francini, S., D’Amico, G., Vangi, E., Borghi, C., Chirici, G., 2022b. Integrating GEDI and Landsat: spaceborne lidar and four decades of optical imagery for the analysis of forest disturbances and biomass changes in Italy. 2022 Sensors 22. <https://doi.org/10.3390/s22052015>, 2015.
- Frate, L., Carranza, M.L., Garfi, V., Di Febbraro, M., Toni, D., Marchetti, M., Ottaviano, M., Santopoli, G., Chirici, G., 2015. Spatially explicit estimation of forest age by integrating remotely sensed data and inverse yield modeling techniques. iForest 9, 63–71. <https://doi.org/10.3832/ifor1529-008>
- Giannetti, F., Puletti, N., Quatrini, V., Travaglini, D., Bottalico, F., Corona, P., Chirici, G., 2018. Integrating terrestrial and airborne laser scanning for the assessment of single-tree attributes in Mediterranean forest stands. Eur. J. Remote Sens. 51, 795–807. <https://doi.org/10.1080/22797254.2018.1482733>
- Gorelick, N., Hancher, M., Dixon, M., Ilyushchenko, S., Thau, D., Moore, R., 2017. Google Earth Engine: Planetary-scale geospatial analysis for everyone. Remote Sens. Environ. 202, 18–27. <https://doi.org/10.1016/j.rse.2017.06.031>
- Griffiths, P., van der Linden, S., Kuemmerle, T., Hostert, P., 2013. A pixel-based Landsat compositing algorithm for large area land cover monitoring. IEEE J. Sel. Top. Appl. Earth Obs. Rem. Sens. 6(5), 2088–2101. <https://doi.org/10.1109/JSTARS.2012.2228167>
- Hansen, M.C., Potapov, P.V., Moore, R., Hancher, M., Turubanova, S.A., Tyukavina, A., Thau, D., et al., 2013. High-resolution global maps of 21st-century forest cover change. Science 342 (6160), 850–853. <https://doi.org/10.1126/science.1244693>. American Association for the Advancement of Science.
- Harris, N.L., Gibbs, D.A., Baccini, A., Birdsey, R.A., de Bruin, S., Farina, M., Fatoyinbo, L., et al., 2021. Global maps of twenty-first century forest carbon fluxes. Nat. Clim. Change 11, 234–240. <https://doi.org/10.1038/s41558-020-00976-6>
- Hollaas, M., Dorigo, W., Wagner, W., Schadauer, K., Höfle, B., Maier, B., 2009. Operational wide-area stem volume estimation based on airborne laser scanning and national forest inventory data. Int. J. Rem. Sens. 30, 5159–5175. <https://doi.org/10.1080/01431160903022894>
- Houghton, R.A., Nassikas, A.A., 2017. Global and regional fluxes of carbon from land use and land cover change 1850–2015. Global Biogeochem. Cycles 31 (3), 456–472.
- Immlitzer, M., Stepper, C., Böck, S., Straub, C., Atzberger, C., 2016. Forest ecology and management use of WorldView-2 stereo imagery and national forest inventory data for wall-to-wall mapping of growing stock. For. Ecol. Manag. 359, 232–246. <https://doi.org/10.1016/j.foreco.2015.10.018>
- INFC, 2021. Italian Forests. Selected Results of the Third National Forest Inventory, ISBN 978-88-338-5140-2. INFC 2015. Carabinieri Command of Forestry, Environmental and Agri-food units and CREA - Research Centre for Forestry and Wood. Tipografia Supernova (TN). Settembre 2021.
- IPCC, 2006. In: Eggleston, H.S., Miwa, K., Srivastava, N., Tanabe, K. (Eds.), IPCC Guidelines for Greenhouse Gases Inventory. A Primer, Prepared by the National Greenhouse Gas Inventories Programme. IGES, Japan.
- ISPRA, 2021a. Moving to the 2006 IPCC Guidelines for UNFCCC Reporting. ISPRA Rapporti 358/2021.
- ISPRA, 2021b. National Inventory Report 2021 - Italian Greenhouse Gas Inventory 1990–2019. ISPRA Rapporti 341/2021.
- Italian Ministry for the Environment, Land and Sea (IMELS), 2019. National Forestry Accounting Plan. Dicember 2019. https://www.minambiente.it/sites/default/files/archivio/allegati/clima/nfap_final_resubmission_2019_clean.pdf.
- Kangas, A., Astrup, R., Breidenbach, J., Fridman, J., Gobakken, T., Korhonen, K.T., Maltamo, M., Nilsson, M., Nord-Larsen, T., Naesset, E., et al., 2018. Remote sensing and forest inventories in Nordic countries—roadmap for the future, 2018 Scand. J. For. Res. 33, 397–412.
- Kavzoglu, T., Colkesen, I., 2009. A kernel functions analysis for support vector machines for land cover classification. Int. J. Appl. Earth Obs. Geoinf. 11 (5), 352–359. <https://doi.org/10.1016/j.jag.2009.06.002>
- Kulbokas, G., Jurevičienė, V., Kuliešis, A., Augustaitis, A., Petrauskas, E., Mikalajūnas, M., Vitas, A., Mozgeris, G., 2019. Fluctuations in gross volume increment estimated by the Lithuanian National Forest Inventory compared with annual variations in single tree increment. Balt. For. 25 (2), 273–280.
- Liaw, A., Wiener, M., 2002. Classification and regression by randomForest. Nucleic Acids Res. 5, 983–999. <https://doi.org/10.1023/A:1010933404324>.

- McRoberts, R.E., Tomppo, E.O., 2007. Remote sensing support for national forest inventories. *Remote Sens. Environ.* 110, 412–419. <https://doi.org/10.1016/j.rse.2006.09.034>.
- McRoberts, R.E., Næsset, E., Gobakken, T., 2013. Accuracy and precision for remote sensing applications of nonlinear model-based inference. *IEEE Journal of Selected Topics in Applied Earth Observations and Remote* 6, 27–34. <https://doi.org/10.1109/JSTARS.2012.2227299>.
- McRoberts, R.E., Chen, Q., Domke, G.M., Ståhl, G., Saarela, S., Westfall, J.A., 2016. Hybrid estimators for mean above-ground carbon per unit area. *For. Ecol. Manag.* 378, 44–56.
- McRoberts, R.E., Næsset, E., Gobakken, T., Chirici, G., Condes, S., Hou, Z., Saarela, S., Chen, Q., Ståhl, G., Walters, B.F., 2018. Assessing components of the model-based mean square error estimator for remote sensing assisted forest applications. *Can. J. For. Res.* 48, 642–649. <https://doi.org/10.1139/cjfr-2017-0396>.
- Mountrakis, G., Im, J., Ogole, C., 2011. Support vector machines in remote sensing: a review, 2011 *ISPRS J. Photogrammetry Remote Sens.* 66, 247–259. <https://doi.org/10.1016/j.isprsjprs.2010.11.001>.
- Næsset, E., Gobakken, T., Holmgren, J., Hyppä, H., Hyppä, J., Maltamo, M., Nilsson, M., Olsson, H., Persson, Å., Söderman, U., 2004. Laser scanning of forest resources: the nordic experience. *Scand. J. For. Res.* 19, 482–499. <https://doi.org/10.1080/08287580410019553>.
- Nilsson, M., Nordkvist, K., Jonzén, J., Lindgren, N., Axensten, P., Wallerman, J., Egberth, M., Larsson, S., Nilsson, S., Eriksson, J., Olsson, H., et al., 2017. A nationwide forest attribute map of Sweden predicted using airborne laser scanning data and field data from the National Forest Inventory. *Remote Sens. Environ.* 194, 447–454. <https://doi.org/10.1016/j.rse.2016.10.022>.
- Nonini, L., Fiala, M., 2021. Estimation of carbon storage of forest biomass for voluntary carbon markets: preliminary results. *J. For. Res.* 32 (1), 329–338. <https://doi.org/10.1007/s11676-019-01074-w>.
- Nord-Larsen, T., Schumacher, J., 2012. Estimation of forest resources from a country wide laser scanning survey and national forest inventory data. *Remote Sens. Environ.* 119, 148–157. <https://doi.org/10.1016/j.rse.2011.12.022>.
- Pal, M., Mather, P.M., 2005. Support vector machines for classification in remote sensing. *Int. J. Rem. Sens.* 26 (5), 1007–1011. <https://doi.org/10.1080/01431160512331314083>.
- Paul, T., Kimberley, M.O., Beets, P.N., 2021. Natural forests in New Zealand—a large terrestrial carbon pool in a national state of equilibrium. *Forest Ecosystems* 8 (1), 1–21. <https://doi.org/10.1186/s40663-021-00312-0>.
- Peng, C., 2000. Understanding the role of forest simulation models in sustainable forest management. *Environ. Impact Assess. Rev.* 20 (4), 481–501. [https://doi.org/10.1016/S0195-9255\(99\)00044-X](https://doi.org/10.1016/S0195-9255(99)00044-X).
- Pinna, M., 1970. Contributo alla classificazione del clima d'Italia. *Riv. Geogr. Ital.* 77 (2), 129–152.
- Saatchi, S.S., Harris, N.L., Brown, S., Lefsky, M., Mitchard, E.T., Salas, W., Zutta, B.R., et al., 2011. Benchmark map of forest carbon stocks in tropical regions across three continents. *Proc. Natl. Acad. Sci. USA* 108 (24), 9899–9904.
- Schepaschenko, D., Molchanova, E., Fedorov, S., Karminov, V., Ontikov, P., Santoro, M., See, L., et al., 2021. Russian forest sequesters substantially more carbon than previously reported. *Sci. Rep.* 11 (1), 1–7. <https://doi.org/10.1038/s41598-021-92152-9>.
- Seebach, L., McCallum, I., Fritz, S., Kindermann, G., LeDuc, S., Böttcher, H., Fuss, A., 2012. Choice of forest map has implications for policy analysis: A case study on the EU biofuel target. *Environ. Sci. Policy* 22, 13–24. <https://doi.org/10.1016/j.envsci.2012.04.010>.
- Sellers, P.J., Schimel, D.S., Moore, B., Liu, J., Eldering, A., 2018. Observing carbon cycle-climate feedbacks from space. *Proceedings of the National Academy of Sciences, U.S.A.* 115, 7860–7868. <https://doi.org/10.1073/pnas.1716613115>.
- Smola, A.J., Schölkopf, B., 2004. A tutorial on support vector regression. *Stat. Comput.* 14 (3), 199–222. <https://doi.org/10.1023/B:STCO.0000035301.49549.88>.
- Tabacchi, G., Di Cosmo, L., Gasparini, P., Morelli, S., 2011. *Stima Del Volume E Della Fitomassa Delle Principali Specie Forestali Italiane, Equazioni Di Previsione, Tavole Del Volume E Tavole Della Fitomassa Arborea Epigea*.
- Tomppo, E., Olsson, H., Ståhl, G., Nilsson, M., Hagner, O., Katila, M., 2008. Combining national forest inventory field plots and remote sensing data for forest databases. *Remote Sens. Environ.* 112, 1982–1999. <https://doi.org/10.1016/j.rse.2007.03.032>.
- Tomppo, E., Gschwantner, T., Lawrence, M., McRoberts, R.E., Gabler, K., Schadauer, K., Cienciala, E., et al., 2010. *National Forest Inventories: Pathways for Common Reporting*, vol. 1. European Science Foundation, pp. 541–553.
- UNFCCC, 2015. The Paris Agreement. Report of the Conference of the Parties on its Twenty-First Session held in Paris from 30 November to 11 December 2015. http://unfccc.int/files/meetings/paris_nov_2015/application/pdf/paris_agreement_english.pdf.
- Van Der Werf, G.R., Randerson, J.T., Giglio, L., Van Leeuwen, T.T., Chen, Y., Rogers, B.M., Kasibhatla, P.S., et al., 2017. Global fire emissions estimates during 1997–2016. *Earth Syst. Sci. Data* 9 (2), 697–720. <https://doi.org/10.5194/essd-9-697-2017>.
- Vangi, E., D'Amico, G., Francini, S., Giannetti, F., Lasserre, B., Marchetti, M., McRoberts, R.E., Chirici, G., 2021. The effect of forest mask quality in the wall-to-wall estimation of growing stock volume. *Rem. Sens.* 13, 1038. <https://doi.org/10.3390/rs13051038>.
- Vizzarri, M., Chiavetta, U., Chirici, G., Garfi, V., Bastrup-Birk, A., Marchetti, M., 2015. Comparing multisource harmonized forest types mapping: A case study from central Italy. *Iforest-Biogeosci. For.* 8, 59–66. <https://doi.org/10.3832/ifor1133-007>.
- Waser, L.T., Ginzler, C., Rehush, N., 2017. Wall-to-Wall tree type mapping from countrywide airborne remote sensing surveys. *Rem. Sens.* 9 <https://doi.org/10.3390/rs9080766>.
- White, J.C., Coops, N.C., Wulder, M.A., Vastaranta, M., Hilker, T., Tompalski, P., 2016. Remote sensing technologies for enhancing forest inventories: a review. *Can. J. Rem. Sens.* 42 (5), 619–641. <https://doi.org/10.1080/07038992.2016.1207484>.
- Williams, P.A., Allen, C., Macalady, A., Griffin, D., Woodhouse, C.A., Meko, D.M., Swetnam, T.W., et al., 2012. Temperature as a potent driver of regional forest drought stress and tree mortality. *Nat. Clim. Change* 3, 292–297. <https://doi.org/10.1038/nclimate1693>.
- Wolfe, R., Masek, J., Saleous, N., Hall, F., 2004. LEDAPS: mapping North American disturbance from the Landsat record. In: *IGARSS 2004. 2004 IEEE International Geoscience and Remote Sensing Symposium*, vol. 1. IEEE.
- Xu, L., Saatchi, S.S., Yang, Y., Yu, Y., Pongratz, J., Bloom, A.A., Bowman, C., et al., 2021. Changes in global terrestrial live biomass over the 21st century. *Sci. Adv.* 7 (27), eabe9829 <https://doi.org/10.1126/sciadv.abe9829>.